

RSC Advances



This is an *Accepted Manuscript*, which has been through the Royal Society of Chemistry peer review process and has been accepted for publication.

Accepted Manuscripts are published online shortly after acceptance, before technical editing, formatting and proof reading. Using this free service, authors can make their results available to the community, in citable form, before we publish the edited article. This *Accepted Manuscript* will be replaced by the edited, formatted and paginated article as soon as this is available.

You can find more information about *Accepted Manuscripts* in the [Information for Authors](#).

Please note that technical editing may introduce minor changes to the text and/or graphics, which may alter content. The journal's standard [Terms & Conditions](#) and the [Ethical guidelines](#) still apply. In no event shall the Royal Society of Chemistry be held responsible for any errors or omissions in this *Accepted Manuscript* or any consequences arising from the use of any information it contains.

**Iron-based Metal-Organic Framework, Fe(BTC): An Effective Two-
Function Catalyst for Oxidative Cyclization of Bisnaphthols and Tandem
Synthesis of Quinazolin-4(3*H*)-ones**

Ali Reza Oveisi, Ahmad Khorramabadi-zad,* and Saba Daliran

Faculty of Chemistry, Bu-Ali Sina University, Hamedan, Iran

*Corresponding author: P.O. Box: 6517838683; Phone: +989188130018; Fax: +98(81)38257407; E-mail address:

khoram@gmail.com (Ahmad Khorramabadi-zad)

Abstract

Iron-based metal-organic framework [Fe(BTC) (BTC: 1,3,5-benzenetricarboxylate)] have been shown to be an active and heterogeneous catalyst for both oxidative cyclization of methylenebisnaphthols and a modern tandem process (an *in situ* oxidation-aminal formation-oxidation sequence). Such a potential catalytic utility of Fe(BTC) make it quite attractive for sustainable industrial chemistry.

Introduction

Calixarenes are synthetic macrocyclic compounds consisting of methylenebisnaphthol or bisphenol skeletons interconnected by methylene bridges.¹ Oxidation of calixarenes can afford bis(spirodienone) derivatives, which are attractive intermediates in forming functionalized calixarenes.² Although, several efforts for the oxidation of methylenebisnaphthols to the corresponding spirodienones have been performed in the presence of different reagents such as DDQ,^{3a} phenyltrimethylammonium tribromide (PTMATB) or Br₂,^{3b} (diacetoxyiodo)benzene in benzene,^{3c} Ph₃Bi,^{3d} Chloramine-T or *N*-chlorosuccinimide,^{3e} *N*-hydroxyimides^{3f} and magnetic core-shell nanoparticle-supported TEMPO (2,2,6,6-tetramethylpiperidine-oxy),^{3g} the use of environmentally benign, inexpensive reagents, milder reaction conditions, and decrease of byproducts are highly demanded.

Quinazolinones and their derivatives have been investigated as biologically active molecules exhibiting a wide range of pharmacological and biological activities such as antitumor, anticonvulsant, antidiabetic and other anticipated activities.⁴ Recently, several synthetic methodologies employing different types of catalysts such as I₂,^{5a} iridium,^{5b} ruthenium,^{5c} and α -MnO₂^{5d} have been reported for the preparation of quinazolin-4(3*H*)-ones. These methods have

some drawbacks such as the use of toxic and/or expensive catalysts or reaction media, not easily available reagents, additives, tedious procedure, and time-consuming.

In recent years, a new class of porous materials such as metal-organic frameworks (MOFs) and porous organic polymers (POPs) have been deeply attracted due to their potential in applications such as chemical catalysis,⁶ gas adsorption,⁷ sensing,⁸ conductivity⁹ and light harvesting sensitizer in solar cells.¹⁰ Metal-organic frameworks are porous crystalline hybrid materials, which are constructed from organic struts and inorganic vertices (metal ions or clusters).^{6c, 11} Iron-based metal-organic framework Fe(BTC) also known as Basolite F300, produced by BASF, has a semi-amorphous structure, a Brunauer-Emmett-Teller (BET) surface area of 1300-1600 m²/g with the same chemical composition of MIL-100(Fe).¹² The latter is comprised of BTC ligands coordinated to iron octahedra [(Fe₃-μ₃O) sharing a common vertex μ₃O]; this iron octahedra contain coordinatively unsaturated metal sites (CUSs) participating in catalytic activities. However, it is reasonable to expect that both Fe(BTC) and MIL(100)-Fe frameworks, have probably the same building units, which can serve to activate substrates for chemical catalysis.^{12a} Iron-based MOF particularly Fe(BTC) have been used for some reactions such as Friedel–Crafts type reactions,^{12b} ring-opening of styrene oxide with methanol and aniline,^{13a} Knoevenagel condensation,^{13b} hydroxyalkylation reaction,^{13b} aerobic oxidation of thiols to disulfides,^{13c} and synthesis of nitriles.^{13d}

Although, many studies have been conducted on catalytic activity of metal-organic frameworks,^{12a, 13-14} only a small number of reports have explored their application in oxidative cyclization and tandem reactions.^{6d, 15}

Our interest in oxidative cyclization of bisnaphthols,^{3d-g} quinazolinones^{6a,16} synthesis and porous materials,^{6a} motivated us to assay further the catalytic potential of metal-organic framework

Fe(BTC) for the oxidative cyclization of methylenebisnaphthols to the corresponding spirodienones and a tandem process (an *in situ* oxidation-aminal formation-oxidation sequence) for the conversion of benzyl alcohols to quinazolin-4(3*H*)-ones.

Results and discussion

Initial studies were carried out using Fe(BTC) as catalyst for the oxidative cyclization of bis(2-hydroxy-1-naphthyl)methane, as a model reaction, in different oxidation conditions (Table 1). It should be noted that Fe(BTC) was activated at 150 °C for 3 h prior to performing these reactions. The oxidation cyclization reaction did not proceed in the presence and absence of Fe(BTC) and 2,2,6,6-tetramethylpiperidine-1-oxyl (TEMPO, a stable free nitroxyl radical)¹⁷ (Table 1, Entries 1-3). As indicated in Table 1, the best oxidant was proven to be hydrogen peroxide (Entries 4-8). The optimum amount of catalyst was found to be 15 mg (3.75 mg of iron from inductively coupled plasma (ICP) analysis. 0.067 mmol of Fe) (Table 1, Entry 6). Carrying out the reaction at room temperature yielded the desired product in 30% after 12 h (Table 1, Entry 7). We have also investigated the effect of solvent (ethanol, acetonitrile, dichloromethane and ethanol/water) and hence, acetonitrile was chosen as the best one (Table 2), affording the highest yield (82%) of the product with less time-consuming than that ethanol and ethanol/water ones, probably because it is relatively inert toward oxidation in the course of oxidation reactions. Also it should be noted that acetonitrile is relatively a green solvent as compared with dichloromethane.

Table 1

Table 2

Having completed the optimization conditions, we were encouraged to examine the oxidative cyclization reaction on a range of bis(2-hydroxy-1-naphtyl)methane derivatives (Table 3). As shown in Table 3, spirodienone derivatives bearing electron-withdrawing and electron-donating substituents were obtained in reasonable yields. Each product was comprised of two sets of diastereomers in nearly equal amounts, assigned by their ^1H NMR spectra because of the different anisotropic shielding effect of the μ -phenyl ring on vinylic H-3' of two diastereomers; **1** and **2**.^{3d,3e,3g}

Table 3

A test for reusability of Fe(BTC) catalyst was then performed using oxidative cyclization of bis(2-hydroxy-1-naphtyl)methane, as a model reaction. After each run, the catalyst was removed by centrifugation and washed with acetonitrile, ethyl acetate, and then acetone followed by drying at 150 °C. Fe(BTC) was reused for three cycles with a little loss in its efficiency (a yield of 76% and 68% of product was obtained after the second and third cycles, respectively), due to some blocked sites by chemicals or partially damage of Fe(BTC) network (Table S1). Atomic absorption spectroscopy (AAS) analysis of supernatant, at the end of reaction, showed 0.3 ppm Fe leaching out which is less than 0.01% of the initial Fe present in the catalyst (0.13 and 0.17 ppm for the second and the third cycles, respectively). Hence, hot-filtration based leaching test was carried out to understand the nature of active species of catalyst in the reaction. Therefore, Fe(BTC) catalyst was removed from the reaction mixture after 4 h, while the supernatant ran further under the same

conditions. There was almost no further yield of spirodienone, even after 8 h in the absence of catalyst (See Table S1 in Electronic Supplementary Material (ESI)). Thus, the results confirmed heterogeneity of the participated catalyst.

Powder X-ray diffraction (PXRD) patterns of the Fe(BTC) exhibit semi-amorphous nature of the matter, resulting in relatively broad or overlapping peaks because of the small size of crystals and its disordered structure (Fig. 1); its characterization by XRD being therefore limited, and no crystal structural data of Fe(BTC) have yet been reported.

To get further information, we compare the PXRD patterns of fresh Fe(BTC) with the simulated crystalline MIL-100(Fe) one (Fig. S1 & S2). As illustrated in Fig 1 and reported in literature,^{12a, 12b, 18} Fe(BTC) shows a broad diffraction peak at low angle, $2\theta \sim 3.6^\circ$ with d spacing of 21.9 Å. The value is in agreement with the 220, 311 and 222 reflections observed in MIL-100(Fe), suggesting the presence of some mesopores cages in the Fe(BTC) [Strong peaks at low angle ($2\theta = 2-4^\circ$)¹⁹ XRD patterns manifest the presence of mesoporous structure], consistent with pore diameter 21 Å obtained from nitrogen adsorption measurements.^{12a,13} Moreover, no diffraction peak appeared in PXRD pattern of Fe(BTC) with d spacing of 42.3 Å, $2\theta \sim 2.0^\circ$, corresponding to the 111 reflection, characteristic of the largest mesopores cages (the largest d spacing of the structure, pore diameter of 29 Å) in MIL-100(Fe). However, the XRD patterns indicate that Fe(BTC) contain just the smallest mesopores cages established in the MIL-100(Fe). Also, a broad peak ($2\theta \sim 10.6^\circ$) shown in the PXRD patterns of Fe(BTC) correlates with the 822, 840 and 911 reflections of observed in MIL-100(Fe).

Comparison of the PXRD of the fresh and the reused catalyst indicates some decrease in the peak intensity of the reused Fe(BTC), suggesting an increase of disordering in the structure or a change in the mesopores content (pore-filling effect) (as shown in Fig. 1, fresh and reused Fe(BTC)-B).

Also Fig.1 shows a slight shift of the main peak positions of the XRD, after reusing, to lower 2θ values (larger d-spacing), suggesting that there is an expansion of the framework in response to the chemicals. It might be attributed to the strain effect of the framework upon strong coordination of reactants or products within the MOF during the reaction. This is consistent with breathing effect in MOFs.²⁰

As scanning electron microscopy (SEM) images shows (Fig. 2), the morphology of the Fe(BTC) was retained under the reaction conditions. SEM images of Fe(BTC) showed agglomerates of spheroid particles, with particle-size ranging from 45 to 105 nm.

A comparison of the FT-IR (See Fig. S3 & S4) of the fresh and reused (the first and the last cycles) catalyst indicated a slightly higher relative intensity of C=O band about 1710 cm^{-1} for the latter, which may be attributed to small amount of spirodienones or impurity along with the free carboxylic groups, is in agreement with the observed changes in powder XRD patterns.

Fig. 1

Fig. 2

When TEMPO was used as a radical scavenger combined with Fe(BTC) and H_2O_2 , significant decrease was observed in yield of spirodienone (Table 1, Entry 8). This reveals that the reaction proceeds through the formation of radical species.^{12c, 21} Based on literature survey^{3g, 12a, 12c} and this observation, we proposed a mechanism for the oxidative cyclization of methylenebisnaphthols as shown in Scheme 1. At first, hydrogen peroxide molecules coordinate to those Fe(III) sites which are not saturated with the framework carboxylate groups, to give Fe(III)-OOH complexes (**I**).

Then the homolytic cleavage of the peroxidic O-O bond in intermediate (I) produces the active species

(HO-O·, II) followed by abstracting a hydrogen-atom from methylenbisnaphthol to afford radical intermediate (III). Abstraction of another hydrogen atom from (III) result in formation of a diradical intermediate formation (IV), which proceed to give the product. Subsequently, Fe(II) is re-oxidized to Fe(III) active sites via an electron transfer to hydrogen peroxide.

Scheme 1

We next examined the potential catalytic activity of this metal-organic framework for a modern tandem process: quinazolin-4(3*H*)-ones synthesis by the reaction of benzyl alcohols and *o*-aminobenzamide in the presence of oxidant (Table 4 and 5). Owing to optimization conditions, at the outset, benzyl alcohol reacted with *o*-aminobenzamide as a model reaction, which afforded 2-phenylquinazolin-4(3*H*)-one (Table 4). As indicated in Table 4, the use of TBHP (tert-butyl hydroperoxide), as an oxidant, gave a higher yield with respect to hydrogen peroxide (Table 4, Entries 1 and 2). It might be due to instability of H₂O₂ compared with that of TBHP in catalytic reaction conditions. The best results were obtained with DMSO (dimethyl sulfoxide) as solvent (Table 4, Entries 5-8), affording the highest yield (81%) of the product as compared with the other solvents. It should be noted that DMSO could act as a mild oxidant, in addition its solvent role. The amount of Fe(BTC) was optimized to be 15 mg (0.067 mmol Fe) in order to reduce the consumed catalyst and to increase the product yield (Table 4, Entry 5). The effect of temperature on this reaction was also investigated, which showed that the reaction should be performed at 60

°C to get a high yield (Table 4, Entry 5). As indicated in Table 4, the reaction did not proceed by DMSO without TBHP (Table 4, Entry 9).

Table 4

In the next step, the optimal condition for the preparation of quinazolin-4(3*H*)-one derivatives was evaluated. The results showed good versatility of this method for neutral, electron rich and electron deficient groups such as H, Me, OMe, Cl, and NO₂ (Table 5). An additional test was also carried out to examine the reusability of the catalyst, using a model reaction of benzyl alcohol with *o*-aminobenzamide. The Fe(BTC) was found to be an efficient and reusable catalyst, with a slight decrease in its activity (Table 5, Entry 1). AAS analysis of supernatant, at the end of reaction, showed 0.7 ppm Fe leaching out for the reaction, attributing to 0.02% of the initial Fe present in the catalyst. Some decrease in the peak intensity of PXRD pattern of the reused Fe(BTC) was observed as compared with that of fresh Fe(BTC) one (see Fig. 1), suggesting an increase of disordering in the structure or a change in the mesopores content (pore-filling effect).

Table 5

According to literature survey, the catalyst sites are the weak Brønsted acid sites (demonstrated by IR pyridine adsorption,^{12a, 22} which may be contributed to unknown impurities or uncoordinated BTC carboxylic groups), the redox-active^{12c} and Lewis acid^{13a} iron sites. So, this catalyst can act usefully both as acid and redox active sites platform.

Based on literature survey and the above argument, we introduce a mechanism for the tandem process as follows (Scheme 2). At first, the coordination of *t*-BuOOH to the Fe(III) sites afford

t-Bu-OO-Fe(III) species (**A**) which subsequently produces the active species (t-Bu-O-O \cdot , **II**). Then, abstraction of a hydrogen-atom from benzyl alcohol gives a radical intermediate (**C**). As the proposed mechanism shows, three the pathways: (**1**), (**2**) and (**3**) give the aldehyde product (**E**). The pathway (**1**) passes through the carbocation formation with the concomitant reduction of Fe(III) to Fe(II). The pathway (**2**) proceeds via a *gem*-diol-like structure formation, and dehydration. The other pathway involves a hydrogen-atom abstraction from (**C**) by the t-BuOO \cdot and t-BuO \cdot radicals. After that, activated aldehyde reacts with *o*-aminobenzamide to give (**G**), which in turn, afford aminal intermediate. Finally, oxidation of aminal intermediate results in quinazolin-4(3*H*)-one formation followed by oxidation of Fe(II) to Fe(III) accomplishes with an electron transfer to t-BuOOH.

Scheme 2

Conclusion

We have further developed the application of porous iron-based MOF as a heterogeneous and catalytically active species for the oxidative cyclization of methylenebisnaphthols, leading to the corresponding two diastereomers in nearly equal amounts (isomers **1** and **2**), as well as a modern tandem process (an *in situ* oxidation-aminal formation-oxidation sequence) for the conversion of benzyl alcohols to quinazolin-4(3*H*)-ones. The catalyst can usefully act as both acid and redox active sites platform. This work consistently has the advantages such as availability of MOF,

inexpensive catalyst, mild reaction conditions, reasonable yields, and simple experimental procedures.

Acknowledgment

The authors gratefully acknowledge the financial support for this work from the Bu-Ali Sina University, Hamedan, Iran.

Notes and references

[†]During the preparation of this work Wang and et al. published a paper related to quinazolinones synthesis using α -MnO₂ as a catalyst.^{5d}

- (a) P. E. Georghiou, M. Ashram, H. J. Clase and J. N. Bridson, *J. Org. Chem.*, 1998, **63**, 1819-1826; (b) S. Chowdhury and P. E. Georghiou, *J. Org. Chem.*, 2002, **67**, 6808-6811; (c) F. Davis and S. Higson, in *Macrocycles: Construction, Chemistry and Nanotechnology Applications*, John Wiley & Sons, Ltd, Chichester, UK, 2011, ch. 5, pp. 126-189.
- (a) S. E. Biali, *Synlett*, 2003, **1**, 0001-0011; (b) R. L. Varma, V. B. Ganga and E. Suresh, *J. Org. Chem.*, 2007, **72**, 1017-1019; (c) S. B. Nimse and T. Kim, *Chem. Soc. Rev.*, 2013, **42**, 366-386.
- (a) T. R. Kasturi, B. Rajasekhar, G. J. Raju, G. M. Reddy, R. Sivaramkrishnan, N. Ramasubbu and K. Venkatesan, *J. Chem. Soc., Perkin Trans. 1*, 1984, 2375-2382; (b) P. E. Georghiou, M. Ashram, H. J. Clase and J. N. Bridson, *J. Org. Chem.*, 1998, **63**, 1819-1826; (c) D. J. Bennett, F. M. Dean, G. A. Herbin, D. A. Matkin, A. W. Price and M. L. Robinson, *J. Chem. Soc., Perkin Trans. 1*, 1980, 1978-1985; (d) A. Khoramabadi-zad, I. Yavari, A. Shiri and A. Bani, *J. Heterocycl. Chem.*, 2008, **45**, 1351-1358; (e) A. Khoramabadi-zad, A. Shiri, F. Derakhshan-Panah and Z. Salimi, *Mol. Diversity*, 2010, **14**, 829-832; (f) A. Khoramabadi-zad, S. Mohammadi and M. Azadmanesh, *Z. Naturforsch. B*, 2014, **69**, 444-450; (g) A. Khorramabadi-zad, S. Daliran and A. R. Oveisi, *C. R. Chim.*, 2013, **16**, 972-976.
- (a) S. Eguchi, in *Bioactive heterocycles I*, ed. S. Eguchi, Springer-Verlag, Berlin-Heidelberg, Germany, 2006, vol. 6, ch. 2, pp. 113-156; (b) V. Sridharan, P. A. Suryavanshi and J. C. Menéndez, *Chem. Rev.*, 2011, **111**, 7157-7259.

- 5 (a) W. Ge, X. Zhu and Y. Wei, *RSC Adv.*, 2013, **3**, 10817-10822; (b) J. Zhou and J. Fang, *J. Org. Chem.*, 2011, **76**, 7730-7736; (c) A. J. A. Watson, A. C. Maxwell and J. M. J. Williams, *Org. Biomol. Chem.*, 2012, **10**, 240-243; (d) Z. Zhang, M. Wang, C. Zhang, Z. Zhang, J. Lu and F. Wang, *Chem. Commun.*, 2015, **51**, 9205-9207.
- 6 (a) A. R. Oveisi, K. Zhang, A. Khorramabadi-zad, O. K. Farha and J. T. Hupp, *Sci. Rep.*, 2015, **5**, 10621-10628; (b) J. Lee, O. K. Farha, J. Roberts, K. A. Scheidt, S. T. Nguyen and J. T. Hupp, *Chem. Soc. Rev.*, 2009, **38**, 1450-1459; (c) A. Dhakshinamoorthy and H. Garcia, *Chem. Soc. Rev.*, 2014, **43**, 5750-5765; (d) M. H. Beyzavi, N. A. Vermeulen, A. J. Howarth, S. Tussupbayev, A. B. League, N. M. Schweitzer, J. R. Gallagher, A. E. Platero-Prats, N. Hafezi, A. A. Sarjeant, J. T. Miller, K. W. Chapman, J. F. Stoddart, C. J. Cramer, J. T. Hupp and O. K. Farha, *J. Am. Chem. Soc.*, 2015, **137**, 13624-13631; (e) P. Kaur, J. T. Hupp and S. T. Nguyen, *ACS Catal.*, 2011, **1**, 819-835.
- 7 (a) A. M. Fracaroli, H. Furukawa, M. Suzuki, M. Dodd, S. Okajima, F. Gándara, J. A. Reimer and O. M. Yaghi, *J. Am. Chem. Soc.*, 2014, **136**, 8863-8866; (b) X. Zhang, Y.-Z. Zhang, D.-S. Zhang, B. Zhu and J.-R. Li, *Dalton Trans.*, 2015, **44**, 15697-15702; (c) N. Nijem, H. Bluhm, M. L. Ng, M. Kunz, S. R. Leone and M. K. Gilles, *Chem. Commun.*, 2014, **50**, 10144-10147; (d) J. A. Mason, M. Veenstra and J. R. Long, *Chem. Sci.*, 2014, **5**, 32-51.
- 8 (a) X. Zhu, H. Zheng, X. Wei, Z. Lin, L. Guo, B. Qiu and G. Chen, *Chem. Commun.*, 2013, **49**, 1276-1278; (b) Z. Hu, B. J. Deibert and J. Li, *Chem. Soc. Rev.*, 2014, **43**, 5815-5840.
- 9 (a) Y. Shen, X.-F. Yang, H.-B. Zhu, Y. Zhao and W.-S. Li, *Dalton Trans.*, 2015, **44**, 14741-14746; (b) P. Ramaswamy, N. E. Wong and G. K. H. Shimizu, *Chem. Soc. Rev.*, 2014, **43**, 5913-5932.
- 10 (a) D. Y. Lee, E.-K. Kim, C. Y. Shin, D. V. Shinde, W. Lee, N. K. Shrestha, J. K. Lee and S.-H. Han, *RSC Adv.*, 2014, **4**, 12037-12042; (b) D. Y. Lee, I. Lim, C. Y. Shin, S. A. Patil, W. Lee, N. K. Shrestha, J. K. Lee and S.-H. Han, *J. Mater. Chem. A*, 2015, **3**, 22669-22676; (c) H.-J. Son, S. Jin, S. Patwardhan, S. J. Wezenberg, N. C. Jeong, M. So, C. E. Wilmer, A. A. Sarjeant, G. C. Schatz, R. Q. Snurr, O. K. Farha, G. P. Wiederrecht and J. T. Hupp, *J. Am. Chem. Soc.*, 2013, **135**, 862-869.
- 11 J. Liu, L. Chen, H. Cui, J. Zhang, L. Zhang and C.-Y. Su, *Chem. Soc. Rev.*, 2014, **43**, 6011-6061.
- 12 (a) A. Dhakshinamoorthy, M. Alvaro, P. Horcajada, E. Gibson, M. Vishnuvarthan, A. Vimont, J.-M. Grenèche, C. Serre, M. Daturi and H. Garcia, *ACS Catal.*, 2012, **2**, 2060-2065; (b) P. Horcajada, S. Surble, C. Serre, D.-Y. Hong, Y.-K. Seo, J.-S. Chang, J.-M. Grenèche, I. Margiolaki and G. Férey, *Chem. Commun.*, 2007, 2820-2822; (c) A. Dhakshinamoorthy, M. Alvaro and H. Garcia, *J. Catal.*, 2012, **289**, 259-265.
- 13 (a) A. Dhakshinamoorthy, M. Alvaro and H. Garcia, *Chem Eur. J.*, 2010, **16**, 8530-8536; (b) M. Opanasenko, A. Dhakshinamoorthy, J. Čejka and H. Garcia, *ChemCatChem*, 2013, **5**, 1553-1561; (c) A. Dhakshinamoorthy, M. Alvaro and H. Garcia, *Chem. Commun.*, 2010, **46**, 6476-6478; (d) A. Rapeyko, M. J. Climent, A. Corma, P. Concepción and S. Iborra, *ChemSusChem*, 2015, **8**, 3270-3282.
- 14 (a) M. H. Beyzavi, R. C. Klet, S. Tussupbayev, J. Borycz, N. A. Vermeulen, C. J. Cramer, J. F. Stoddart, J. T. Hupp and O. K. Farha, *J. Am. Chem. Soc.*, 2014, **136**, 15861-15864; (b) J. E. Mondloch, M. J. Katz, W. C. Isley III, P. Ghosh, P. Liao, W. Bury, G. W. Wagner, M. G. Hall, J. B. DeCoste, G. W. Peterson, R. Q. Snurr, C. J. Cramer, J. T. Hupp and O. K. Farha, *Nature Mater.*, 2015, **14**, 512-516.

- 15 (a) A. Dhakshinamoorthy and H. Garcia, *ChemSusChem*, 2014, **7**, 2392-2410; (b) Y. Zhang, B. Li and S. Ma, *Chem. Commun.*, 2014, **50**, 8507-8510; (c) G. H. Dang, Y. T. H. Vu, Q. A. Dong, D. T. Le, T. Truong and N. T. S. Phan, *Appl. Catal., A*, 2015, **491**, 189-195.
- 16 (a) H. R. Shaterian and A. R. Oveisi, *Chin. J. Chem.*, 2009, **27**, 2418-2422; (b) H. R. Shaterian, A. R. Oveisi and M. Honarmand, *Synth. Commun.*, 2010, **40**, 1231-1242.
- 17 Q. Cao, L. M. Dornan, L. Rogan, N. L. Hughes and M. J. Muldoon, *Chem. Commun.*, 2014, **50**, 4524-4543.
- 18 G. Majano, O. Ingold, M. Yulikov, G. Jeschke and J. Perez-Ramirez, *CrystEngComm*, 2013, **15**, 9885-9892.
- 19 (a) G. Férey, C. Mellot-Draznieks, C. Serre, F. Millange, J. Dutour, S. Surblé and I. Margiolaki, *Science*, 2005, **309**, 2040-2042; (b) H.-j. Zhang, S.-d. Qi, X.-y. Niu, J. Hu, C.-l. Ren, H.-l. Chen and X.-g. Chen, *Catal. Sci. Technol.*, 2014, **4**, 3013-3024.
- 20 (a) F. Millange, C. Serre, N. Guillou, G. Férey and R. I. Walton, *Angew. Chem. Int. Ed.*, 2008, **47**, 4100-4105; (b) M. H. Alkordi, Y. Liu, R. W. Larsen, J. F. Eubank and M. Eddaoudi, *J. Am. Chem. Soc.*, 2008, **130**, 12639-12641; (c) G. Férey and C. Serre, *Chem. Soc. Rev.*, 2009, **38**, 1380-1399.
- 21 M. O. Ratnikov and M. P. Doyle, *J. Am. Chem. Soc.*, 2013, **135**, 1549-1557.
- 22 C. Volkringer, H. Leclerc, J.-C. Lavalley, T. Loiseau, G. Férey, M. Daturi and A. Vimont, *J. Phys. Chem. C*, 2012, **116**, 5710-5719.

Schemes, Figures, and Tables captions

Table 1 The oxidative cyclization of bis(2-hydroxy-1-naphthyl)methane using Fe(BTC) as heterogenous catalyst

Table 2 The oxidative cyclization of bis(2-hydroxy-1-naphthyl)methane using different types of solvent in the presence of Fe(BTC)

Table 3 The oxidative cyclization of bisnaphthols using Fe(BTC)

Fig. 1 PXRD patterns of a) fresh (activated at 150 °C), b), and d) reused Fe(BTC) in the oxidative cyclization of bis(2-hydroxy-1-naphthyl)methanes (reused Fe(BTC)-B, green) and the quinazoline-4(3*H*)-ones synthesis (reused Fe(BTC)-Q, blue), respectively.

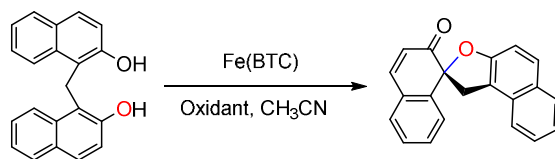
Fig. 2 SEM images of a) fresh and b) reused Fe(BTC)

Scheme 1 Proposed mechanism for the oxidative cyclization of bisnaphthols in the presence of Fe(BTC)

Table 4 Tandem catalytic synthesis of 2-phenylquinazolin-4(3*H*)-one using Fe(BTC)

Table 5 Tandem catalytic synthesis of quinazolin-4(3*H*)-one derivatives using Fe(BTC)

Scheme 2 Proposed mechanism for the quinazoline-4(3*H*)-ones from benzyl alcohols in the presence of Fe(BTC)

Table 1 The oxidative cyclization of bis(2-hydroxy-1-naphthyl)methane using Fe(BTC) as a heterogenous catalyst^a

Entry	Fe(BTC) ^b (mg)	Fe (mol%)	Oxidant	Time (h)	Yield (%) ^c
1	15	13	-	12	-
2	15	13	TEMPO	12	-
3	-	-	H ₂ O ₂	12	trace
4	8	7	H ₂ O ₂	8	55
5	25	22	H ₂ O ₂	7	78
6	15	13	H ₂ O ₂	8	82
7 ^d	15	13	H ₂ O ₂	12	30
8 ^e	15	13	H ₂ O ₂	12	30

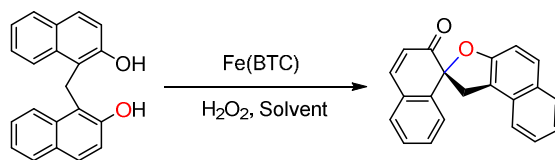
^a Reaction conditions: C₂₁H₁₆O₂ (0.5 mmol), Fe(BTC) as catalyst, oxidant (1.6 mmol, 3.2 eq.), and acetonitrile (5 ml) at 40 °C.

^b Fe(BTC) is contain of 25% of Fe.

^c Total yield (purified by column chromatography).

^d Reaction was carried out in room temperature.

^e 1.5 equiv. of TEMPO was used.

Table 2 The oxidative cyclization of bis(2-hydroxy-1-naphthyl)methane using different types of solvent in the presence of Fe(BTC)

Entry	Solvent	Time (h)	Yield (%)
1	EtOH	10	22
2	EtOH/H ₂ O (30:70)	10	31
3	CH ₂ Cl ₂	8	76
4	CH ₃ CN	8	82

^a Reaction conditions: C₂₁H₁₆O₂ (0.5 mmol), Fe(BTC) (15 mg, 0.067 mmol Fe), H₂O₂ (1.6 mmol), and solvent (5 ml) at 40 °C.

Table 3 The oxidative cyclization of bisnaphthols using Fe(BTC)^a

Fe(BTC)
 $\text{H}_2\text{O}_2, 40\text{ }^\circ\text{C}$
 CH_3CN

Isomer 1 **Isomer 2**

Entry	X	Time (h)	Yield (%) ^b	M.p. (°C)				Diastereomeric ratio (%) ^c	
				Found		Lit [10-13]		1	2
				1	2	1	2		
				1	2	1	2	1	2
1	H	8	82	170-171		170-171		-	-
2	C ₆ H ₅	8	80	209-211	264-266	210-211	263-264	75	25
3	4-CH ₃ C ₆ H ₄	8	76	199-201	228-230	198-200	227-229	50	50
4	3-CH ₃ C ₆ H ₄	10	81	187-189	225-227	187-188	225-227	50	50
5	2-CH ₃ OC ₆ H ₄	7	78	228-231	194-196	229-230	194-196	55	45
6	2,4-Cl ₂ C ₆ H ₃	9	85	208-209	195-197	204-206	195-197	55	45
7	4-FC ₆ H ₄	10	80	214-216	145-146	214-215	145-146	50	50
8	2-BrC ₆ H ₄	8	78	219-221	147-149	218-223	146-148	55	45

^a Reaction conditions: bisnaphthol (0.5 mmol), Fe(BTC) (15 mg, 0.067 mmol Fe), H₂O₂ (1.6 mmol, 3.2 eq.), and acetonitrile (5 ml) at 40 °C.

^b Yield refer to the isolated pure products (isomer **1** + isomer **2**).

^c The ratio of the two diastereomers (isomer **1** and isomer **2**) is distinguished by ¹H NMR.

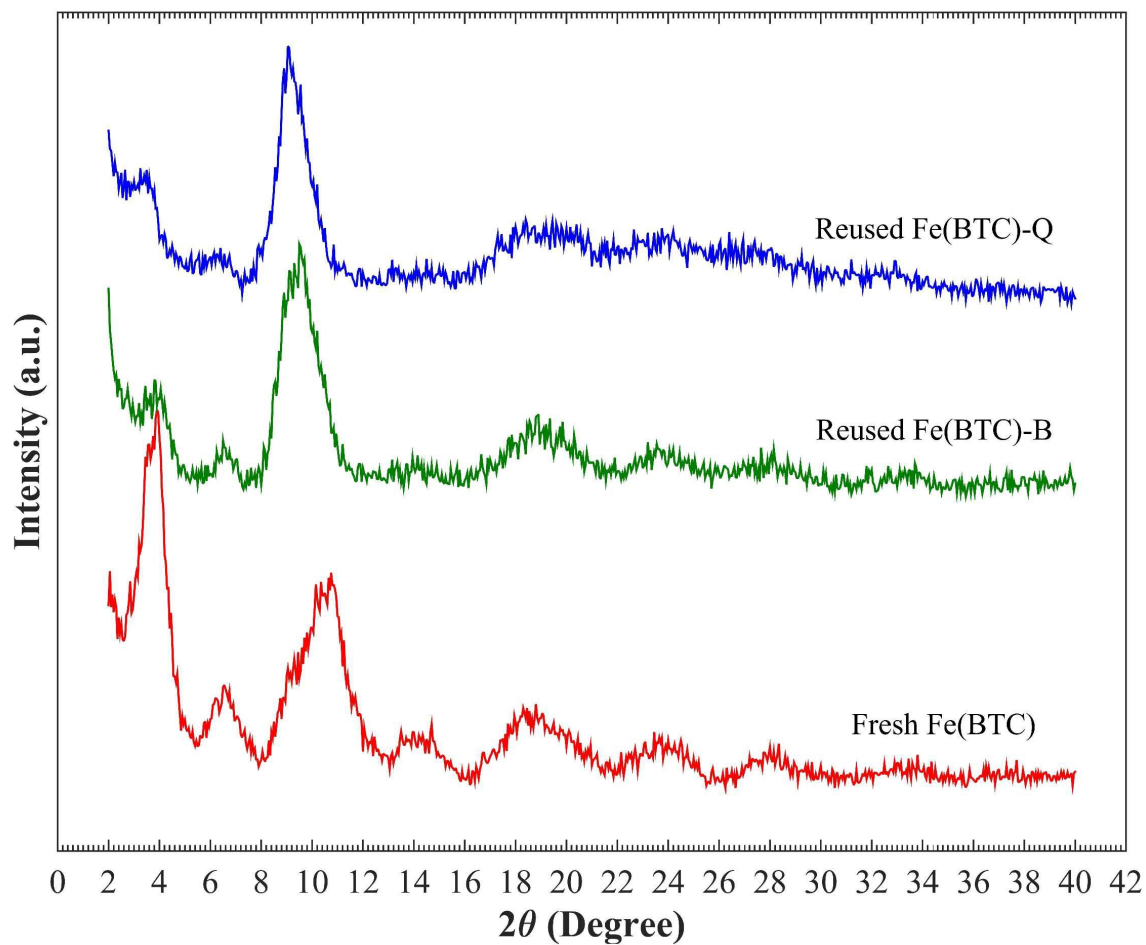


Fig. 1 PXRD patterns of a) fresh (activated at 150 °C, red), b), and d) reused Fe(BTC) in the oxidative cyclization of bis(2-hydroxy-1-naphthyl)methanes (reused Fe(BTC)-B, green) and the quinazoline-4(3*H*)-ones synthesis (reused Fe(BTC)-Q, blue), respectively.

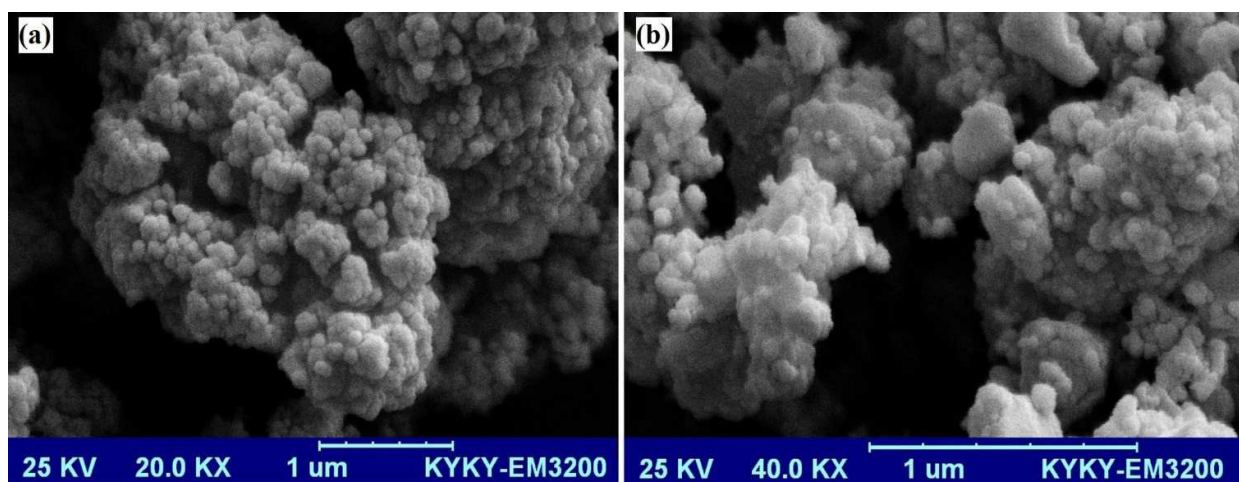
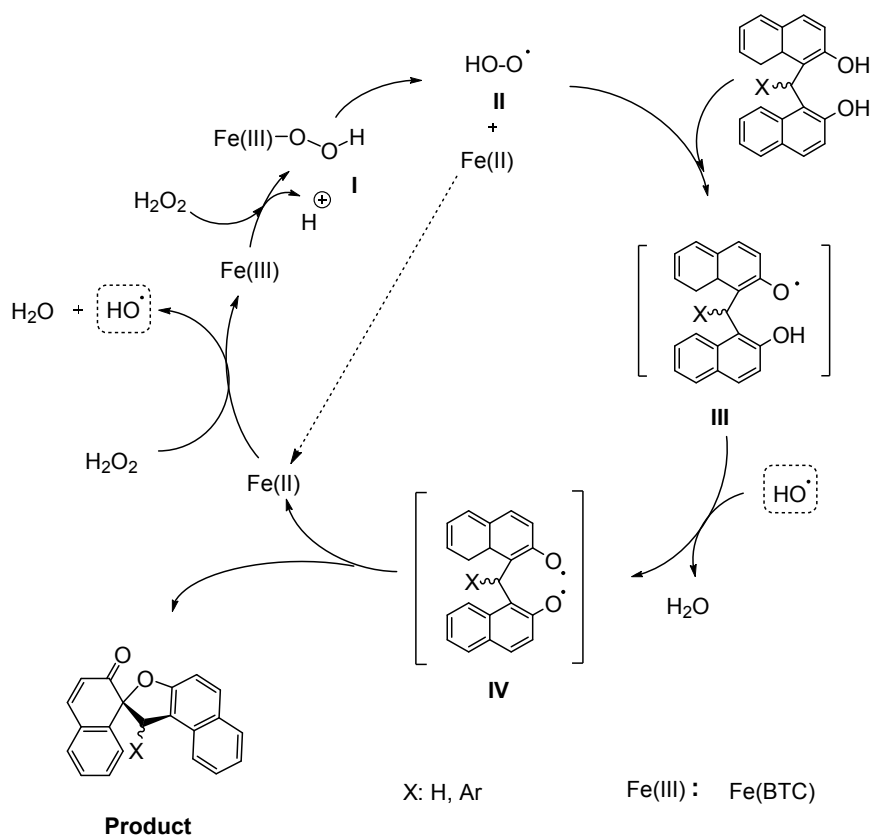
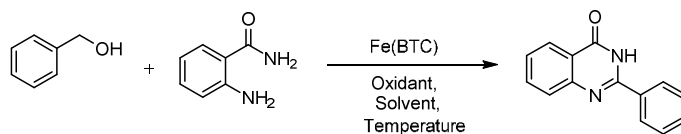


Fig. 2 SEM images of a) fresh and b) reused Fe(BTC)



Scheme 1 Proposed mechanism for the oxidative cyclization of bisnaphthols in the presence of Fe(BTC)

Table 4 Tandem catalytic synthesis of 2-phenylquinazolin-4(3*H*)-one using Fe(BTC)^a

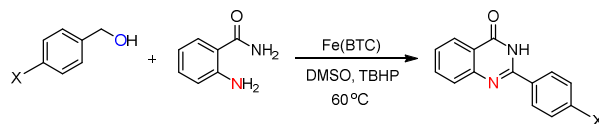
Entry	Fe(BTC) ^b (mg)	Fe (mo%)	Oxidant	T (°C)	Solvent	Time (h)	Yield (%) ^c
1	15	13	H ₂ O ₂	40	CH ₃ CN	14	21
2	15	13	TBHP	40	CH ₃ CN	14	39
3	15	13	TBHP	60	CH ₃ CN	14	47
4	15	13	TBHP	60	Xylene	14	30
5	15	13	TBHP	60	DMSO	14	81
6	15	13	TBHP	85	DMSO	14	78
7	10	9	TBHP	60	DMSO	14	75
8	22	20	TBHP	60	DMSO	14	82
9	15	13	-	60	DMSO	14	-

^a Reaction conditions: benzyl alcohol (1.5 mmol), *o*-aminobenzamide (0.5 mmol), oxidant (2 mmol), solvent (3-5 ml), Fe(BTC) (10-22 mg).

^b 15 mg Fe(BTC) is equal to 3.75 mg Fe (0.067 mmol Fe).

^c Yield refer to the isolated pure products.

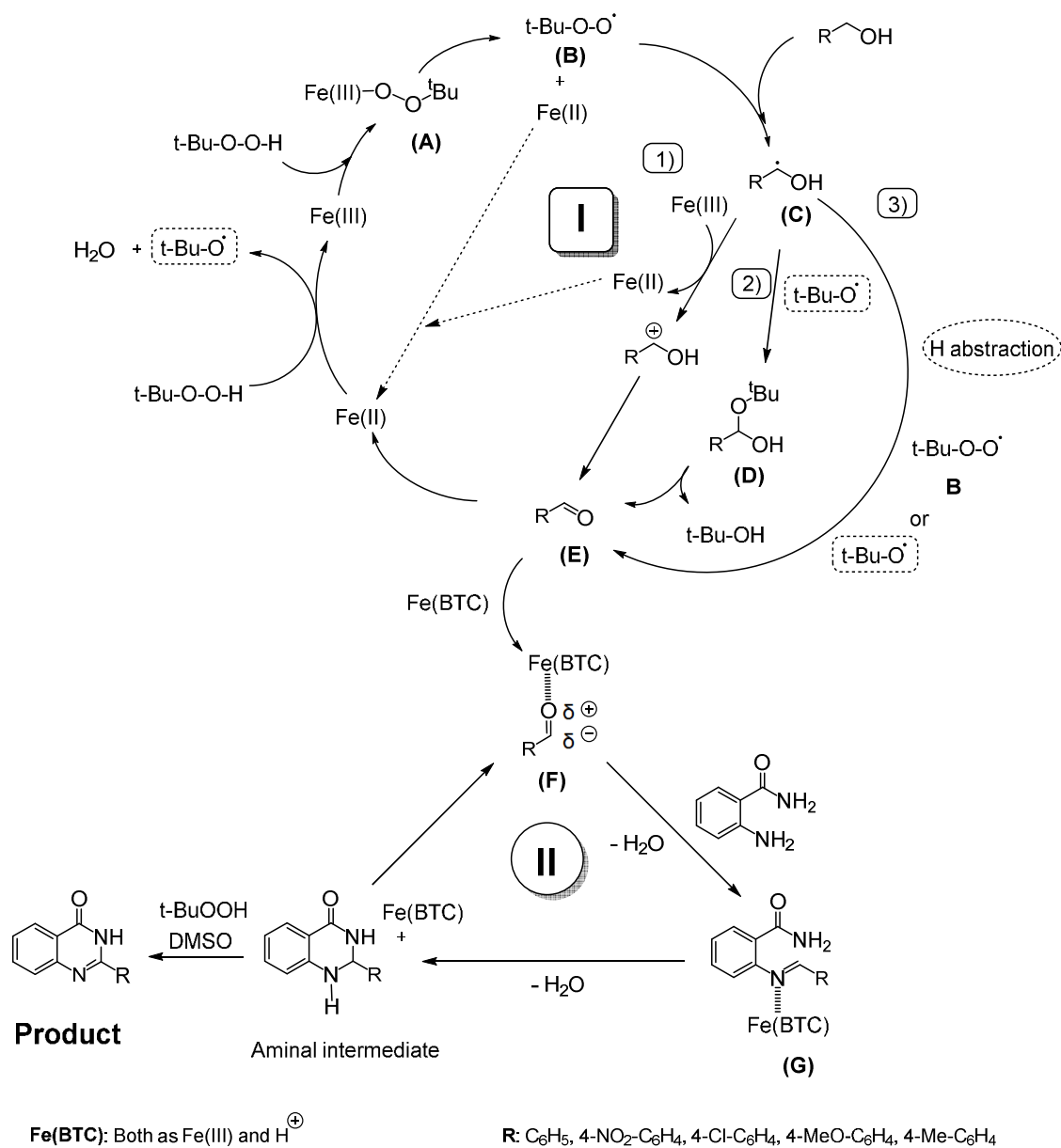
Table 5 Tandem catalytic synthesis of quinazolin-4(3*H*)-one derivatives using Fe(BTC)^a



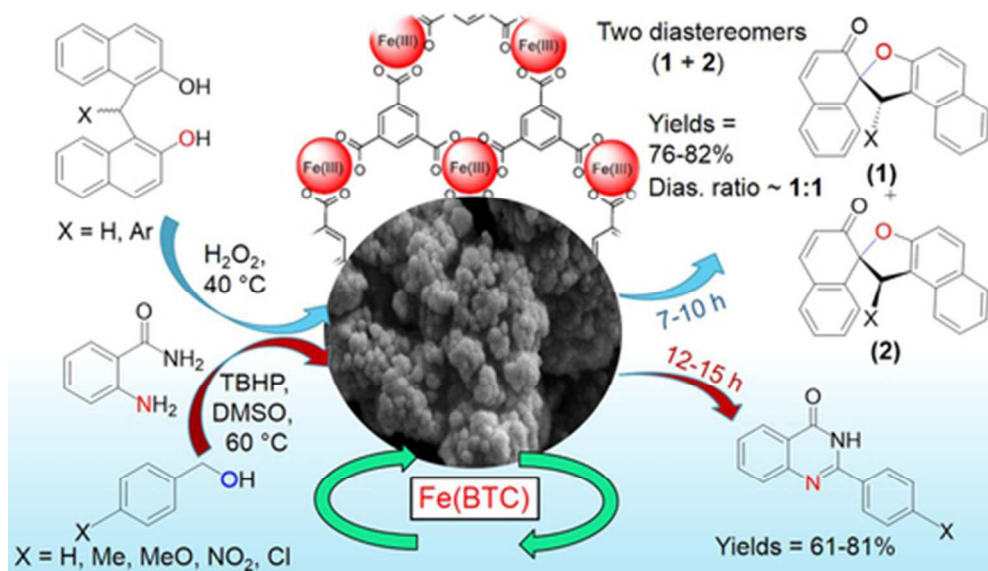
Entry	X	Time (h)	Yield (%)
1	H	14	81, 70 ^b
2	Me	15	74
3	MeO	15	70
4	NO ₂	14	68
5	Cl	12	61

^a Reaction conditions: *o*-aminobenzamide (0.5 mmol)benzyl alcohol (1.5 mmol), TBHP (2 mmol), DMSO (3 ml), Fe(BTC) (15 mg, 0.067 mmol), at 60 °C.

^b Reusability of Fe(BTC) in the second run.



Scheme 2 Proposed mechanism for the quinazoline-4(3*H*)-ones from benzyl alcohols in the presence of Fe(BTC)



Fe(BTC) Catalyzed Synthesis of Spirodienones and Quinazolin-4(3H)-ones
41x23mm (300 x 300 DPI)